Gwyn Griffiths, G3ZIL
14 Bassett Close, Southampton SO16 7PE, UK | **gwyn@autonomousanalytics.com**

Identifying 14 MHz Propagation Modes Using FST4W SNR and Spectral Spread

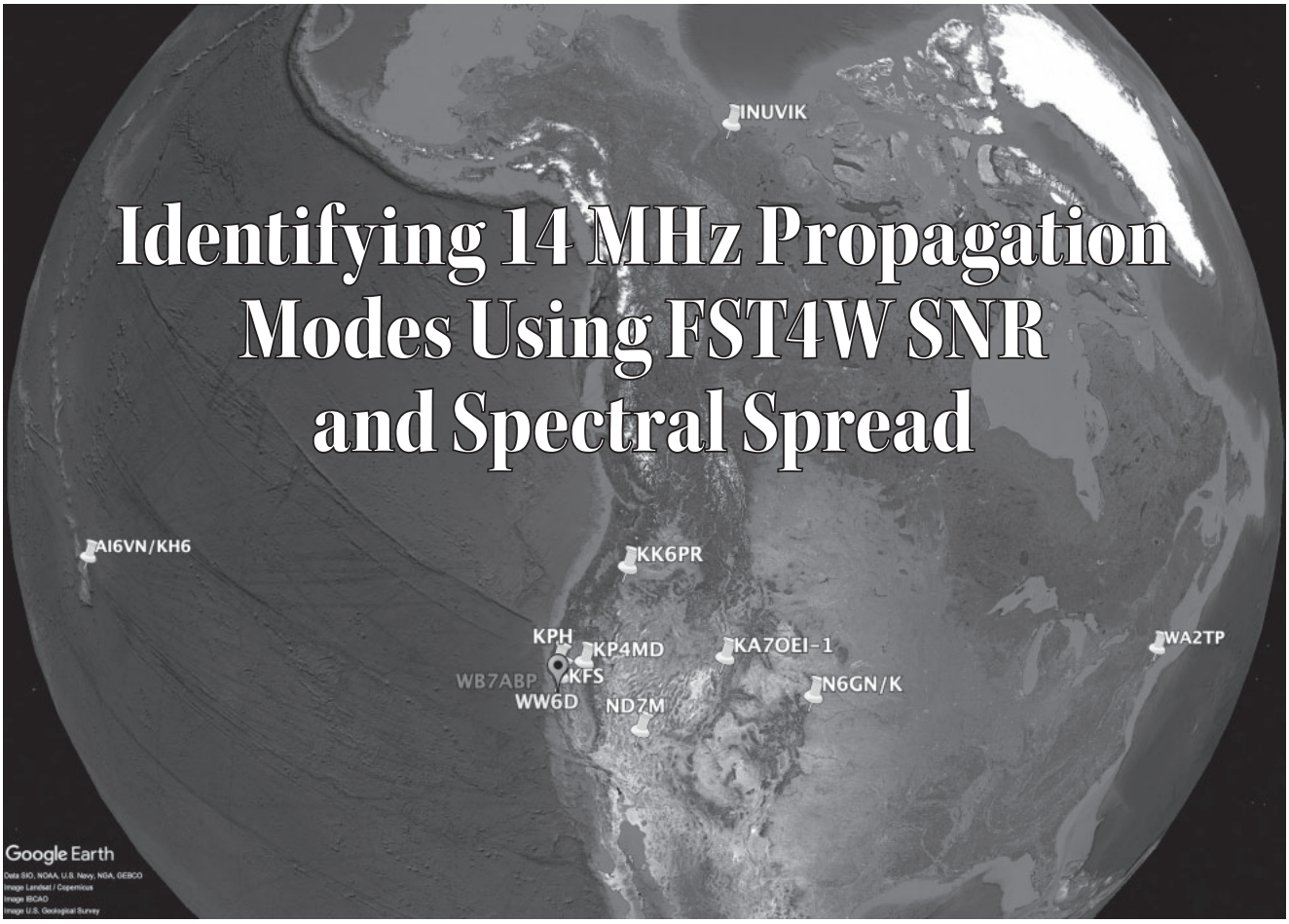

Spectral spread at the transmitter and receiver can be less than 30 mHz with equipment of modest cost.

The FST4W protocol within the WSJT-X family of weak signal communications programs has an advantage over the widely used WSPR protocol in that it estimates spectral spreading. With equipment of modest cost, spectral spread at the transmitter and receiver can be less than 30 mHz. In most circumstances this is lower than spectral spread imposed on signals by single-hop ionospheric refraction at HF. Simple two-dimensional scatter plots of spectral spread and signal to noise ratio, alongside time series plots, show clear clustering attributable to different propagation modes. Using a single FST4W transmitter in Northern California and reports from eleven receivers, from 2.4 km to over 4000 km distant, clusters for ground wave and ionospheric one-hop (1F) and two-hop (2F) paths were easily identifiable. The propagation modes for other clusters were not so obvious. In particular, the prevalence of 2F ground side-scatter, or skew off-great circle propagation, also termed 'above the basic maximum usable frequency' propagation, at ranges of 40 km to 1000 km was unexpected. This mode was also seen after dusk at more distant receivers. It followed on from 1F propagation as the maximum usable frequency fell. Identifying the particular propagation mode over a path may be of interest to radio amateurs. For example, if the prevailing mode is 2F ground side-scatter, antenna headings along a great circle path may not give best results.

Motivation

The original motivation for this study was to try and identify the propagation mechanism for horizontally polarized WSPR

Figure 1 (above) — Map of the locations of the transmitter WB7ABP at Santa Rosa (dark grey) and receivers (white) for the December 2022 experiment. Map courtesy Google Earth.

transmissions on 14 MHz from WB7ABP, Santa Rosa, CA received at KPH, Point Reyes, CA, a distance of about 40 km. Conventional wisdom has it that the horizontally polarized ground wave signals from WB7ABP, received on horizontally polarized antenna at KPH could not have produced the +7 dB SNR in 2.5 kHz that was observed with little variation over 24 hours given the maximum usable frequency at that time for the path length was less than 14 MHz.

The study expanded beyond considering only the 40 km path from WB7ABP to KPH. Three other strands were added. First, we investigated whether the unknown propagation mode was present on other paths. Second, we studied paths where, with certainty, the mechanism was magneto-ionic refraction in the ionosphere F layer. Third, we considered whether the two-parameter method adopted for this study — cluster plots of FST4W SNR and spectral spreading — could identify other propagation mechanisms.

The December 2022 Experiment

The main experiment ran from 1600 UTC 29 December 2022 to 0800 UTC 31 December 2022. The single transmitter was an ANAN-100D at WB7ABP, Santa Rosa, CA. (CM88ok, 38.44° N 122.79° W) with 5 W output to a 5-element horizontally polarized KT-34XA Yagi, with a beamwidth of about 50°, directed northwest. The mode was FST4W-120 with a one-in-three duty cycle. A phase-locked GPSDO master oscillator ensured transmit frequency stability and low spectral spreading. The location is shown as the dark grey map pin in **Figure 1**.

All receivers whose data were used in this experiment were KiwiSDRs running *WsprDaemon* release v3.0.3 or later **[1]** except for an Elad receiver with WSJT-X 2.5.4 at WW6D. *WsprDaemon* acquires and reports additional data fields not sent to the **wsprnet.org** database. These fields include reporting frequency to a resolution of 0.1 Hz and FST4W spectral spreading to the extended spots database **[2]**. Spots from the local receiver WB7ABP/K were used to check that there were no outages in transmissions. The KiwiSDRs were running firmware version 1.557 or later ensuring that the spectral spreading contribution if using the out-of-the-box GPS aiding was on the order of 30 mHz or less. Some sites used a phase-locked GPSDO with their KiwiSDR (N6GN/K, WA2TP). We chose not to use the phase-locked receiver at KFS to show that the results and subsequent interpretation could be done elsewhere with a standard KiwiSDR or equivalent. Receiver locations are the white map pins in **Figure 1**.

A rich set of contrasting paths was possible:

Local group – 0 to 150 km:

- Near field (WB7ABP/K) as a record of transmissions made.
- 2.4 km ground (or surface) wave, line-of-sight except for suburban structures (WW6D).
- 40 km SSW to a coastal site (KPH) at Point Reyes, CA.
- 121 km SSE to a coastal site, partly over seawater (KFS) at Half Moon Bay, CA.
- 133 km NE inland (KP4MD) near Sacramento, CA.

500 – 1525 km, all over land:

- 645 km ESE (ND7M), Nevada.
- 679 km N (KK6PR), Oregon.
- 960 km NE (KA7OEI-1), Northern Utah.
- 1525 km ENE (N6GN/K), Northern Colorado.

Table 1 – Indicators of geomagnetic and solar conditions for 29-31 December 2022. The A index is for Fredericksburg, SSN is sunspot number, solar flux is the standard flux at 10.7 cm, and Kp is the planetary maximum for the day. Data from https://www.swpc.noaa.gov/ and https://spaceweather.com/.

Date	Mid Lat A	Max flare	time UTC	SSN	Solar flux	Kp max
29 Dec	8	M2	18:33	88	160	3
30 Dec	22	M3	19:38	113	163	5
31 Dec	10	C9	21:48	121	162	3.3

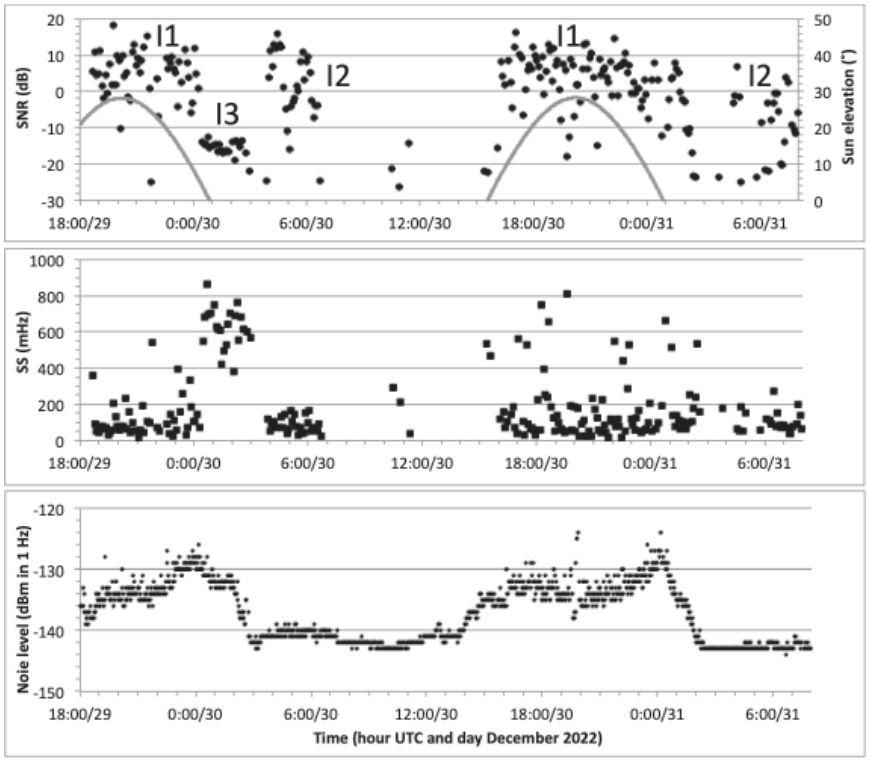

Figure 2 — Time series of (top) SNR and sun elevation angle, (middle) spectral spread for WB7ABP FST4W-120 transmissions received at KA7OEI-1 (Northern Utah SDR site) at a distance of 960 km together with (bottom) noise level.

Paths over 3000 km

- 4210 km, transcontinental, over land, ENE (WA2TP), Long Island, NY.
- 3762 km seawater path except for ~30 km, WSW (AI6VN/KH6), Maui.
- 3392 km into and across the auroral oval, N overland (Inuvik), Northwest Territory, Canada.

The geomagnetic conditions during the experiment, **Table 1**, spanned from quiet to disturbed with M-class solar flares on two days. The smoothed December 2022 sunspot number (SSN) was taken as 103 for use in propagation and ray trace modeling.

Details of FST4W's estimation of spectral spread are available in Griffiths et al. (2022) **[3]**. Unpublished work has shown that while interference from co-channel WSPR signals can affect FST4W SNR and spectral spread the WSPR SNR has to be at least 8 dB above that of the FST4W signal, and overlapping, to produce statistically significant outliers. Using median values in this study avoids possible errors from co-channel interference.

Results

One example time series is shown out of eleven acquired.

Figure 2 is the time series for the 960 km path from WB7ABP to KA7OEI-1, the Northern Utah SDR site. A data report **[4]** is available that includes a full set of time series graphs of the following parameters for each path:

- SNR in dB in a bandwidth of 2.5 kHz superimposed with altitude of the sun at the mid point of a great circle path. The geographical location of receivers was calculated from their grid location and the great circle bearing; distance and mid point were obtained using an online calculator. The mid points were set as variables for each path in the *Grafana* dashboard, as inputs to a Sun and Moon data source plug-in from C. Fetzer **[5]**.
- FST4W spectral spread in mHz, calculated as the frequency span between the 25% and 75% points of the cumulative power distribution with frequency.
- Noise level in dBm in 1 Hz bandwidth at the antenna socket of the KiwiSDR estimated using the FFT method using the total power in the lowest 30% of spectral estimates between 1340 Hz and 1640 Hz at baseband **[6]**. At sites with low local noise the record can show periods when propagated-in noise dominated or was absent.

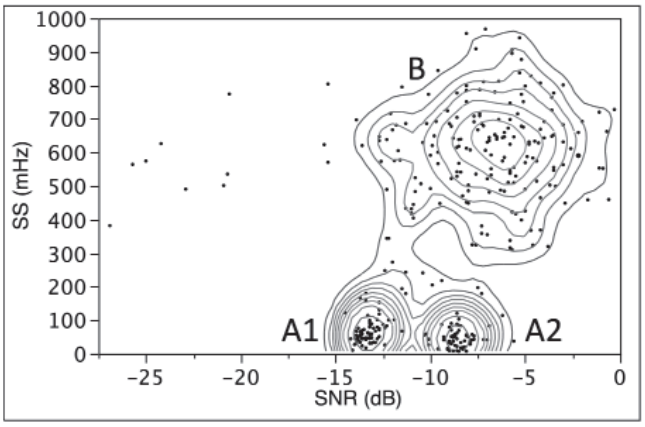

Figure 3 — Scatter plot with density contours of spectral spread and SNR showing distinct separation of the two clusters labeled A (A1 and A2 on the two days) and B at KPH.

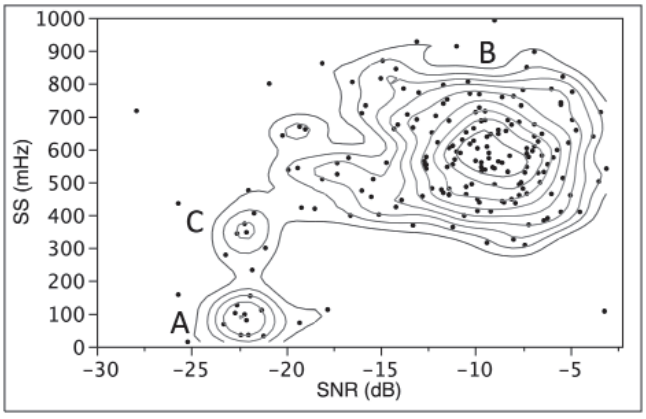

Figure 4 — Scatter plot with density contours of spectral spread and SNR showing distinct separation of the three clusters labeled A, B and C at KFS.

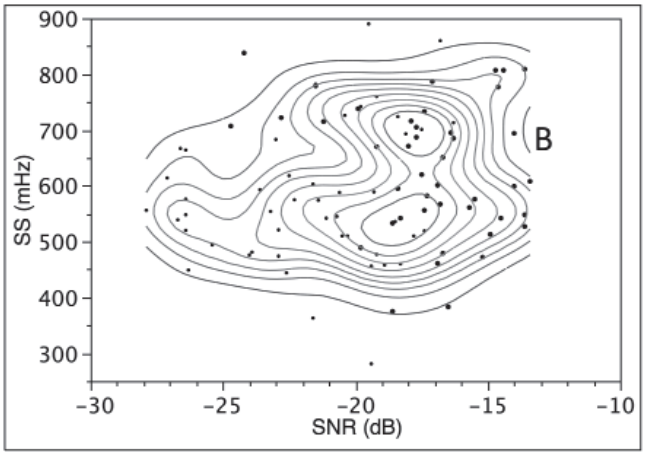

Figure 5 — Scatter plot with density contours of spectral spread and SNR showing the single cluster label B at KP4MD, with two peaks due to day-to-day variability.

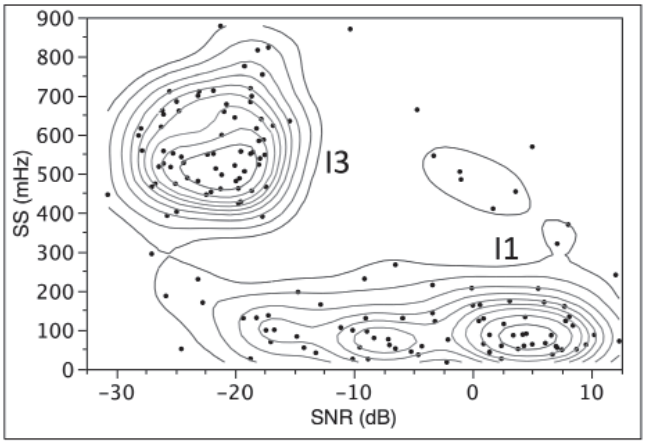

Figure 6 — Scatter plot with density contours of spectral spread and SNR showing distinct separation of the two cluster labeled I1 and I3 at ND7M.

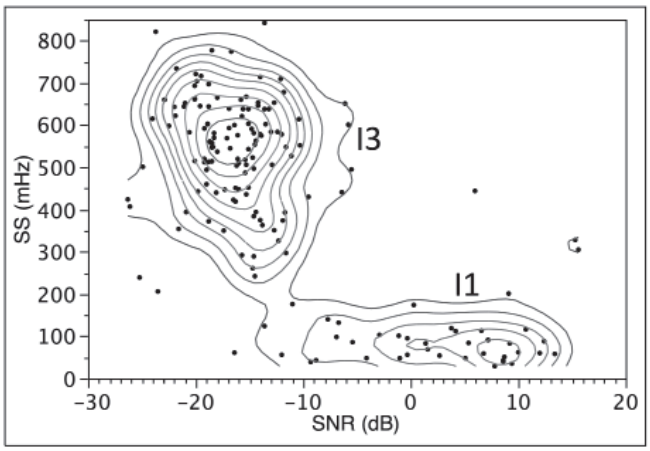

Figure 7 — Scatter plot with density contours of spectral spread and SNR showing distinct separation of the two clusters labeled I1 and I3 at KK6PR.

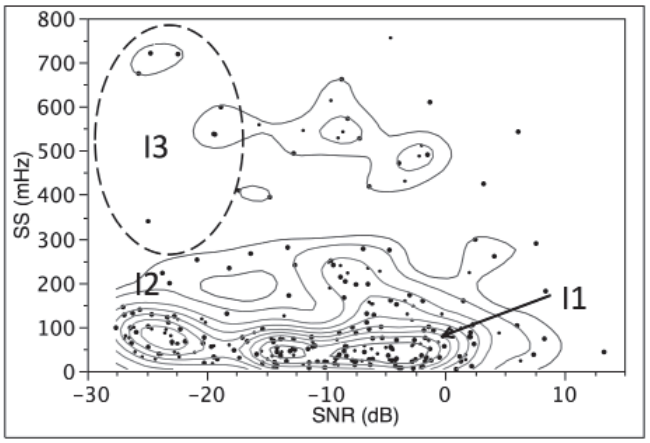

Figure 9 — Scatter plot with density contours of spectral spread and SNR showing distinct separation of the three clusters labeled I1, I2 and I3 at N6GN/K.

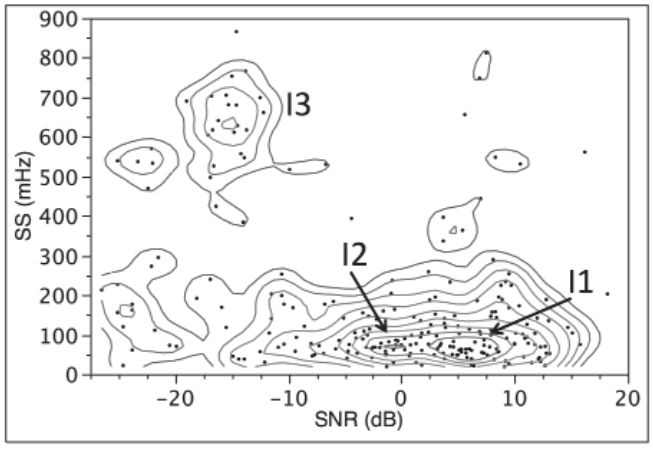

Figure 8 — Scatter plot with density contours of spectral spread and SNR showing modest separation of the two clusters labeled I1 and I2 at KA7OEI-1 with a clear separation from I3.

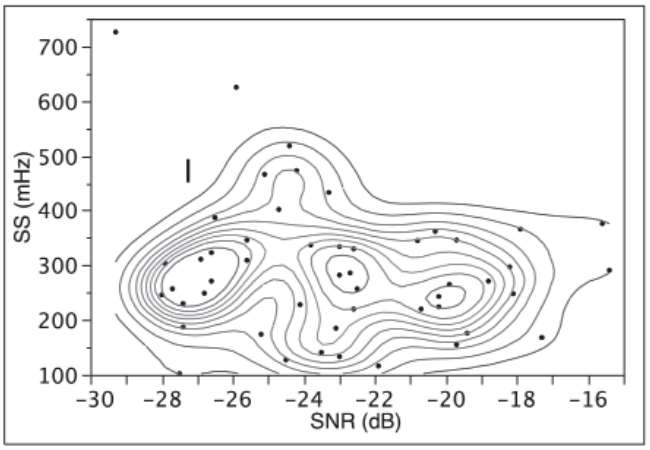

Figure 10 — Scatter plot with density contours of spectral spread and SNR showing a single cluster labeled I with variations in SNR during daily openings at WA2TP.

For each path a scatter plot of spectral spread and SNR was annotated with a label for identifiable clusters (**Figures 3 – 12**):

- G – ground wave at WW6D at 2.4 km, data report [4] only.
- A – uncertain propagation mode, only applicable at KPH and, very briefly, at KFS, with relatively high SNR and low spectral spread; split into A1 and A2 at KPH to show day-to-day variation.
- B – uncertain propagation mode, applicable in the Local Group out to 150 km range, higher SNR than label A but high spectral spread.
- C – only observed at KFS, lower SNR than label B with medium spectral spread.
- I – assessed as various forms of ionospheric propagation, split into I1-I7 where there were distinct patterns to the SNR and spectral spread clusters.

For each path the median and median absolute deviation for SNR and spectral spreading were calculated. Median absolute deviation (MAD) is a more robust estimate of variation where the data distribution may not be Gaussian. While there were day-to-day variations, visible as two or more peaks within a labeled cluster, the separation between labeled clusters was invariably clear. When taken with the time series plots the clusters enabled attribution to propagation mode.

Synthesis

In this section we attempt to attribute the SNR and SS clusters identified at each receiver in **Figures 3 – 12** to particular propagation modes. In several cases we compared received SNR time series to predicted SNR from a point-to-point propagation prediction model. The model used, *Proppy* **[7]**, is an online version of the ITU's *ITURHFPROP* application based on Recommendation ITU-R P.533-14 **[8]** implemented by James Watson, MØDNS. *Proppy* includes WSPR as a traffic option for SNR calculation. Those properties are close enough to FST4W-120 for this study.

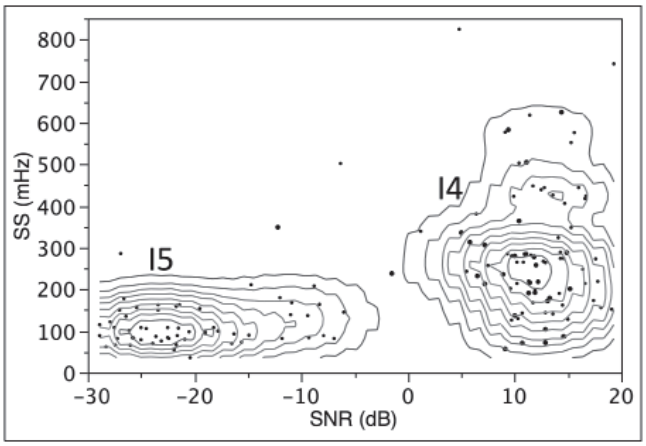

Figure 11 — Scatter plot with density contours of spectral spread and SNR showing distinct separation of the two clusters labeled I4 and I5 at AI6VN/KH6.

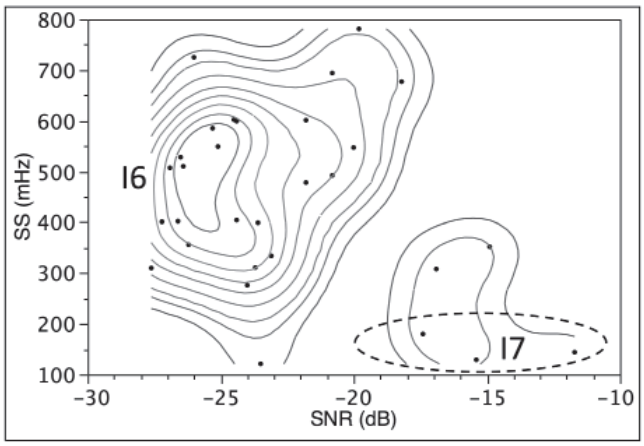

Figure 12 — Scatter plot with density contours of spectral spread and SNR showing two clusters labeled I6 and I7 at INUVIK. The automatic contouring has included spots with higher spectral spread than the true I7 cluster that has been manually determined within the dotted contour.

500 – 1525 km over land

Label I1: Considering first the 960 km path to KA7OEI-1, **Figure 13** shows the measured and *Proppy*-predicted SNR time series. The alignment of I1 with the prediction suggests strongly that the cluster labeled I1, with high SNR and low spectral spreading, was due to single-hop magneto-ionic refraction in the F2 layer, i.e. 1F.

Label I2: For this path I2 was observed during the night, with a median SNR of about 9 dB below the daytime 1F mode and a low spectral spreading, median 28 mHz. Examination of contemporaneous ionosonde profiles at the Idaho National Laboratory (600 km NE of the path mid point, 195 km N of KA7OEI-1) showed that I2 was an example of above-the-MUF propagation as described in McNamara et al. (2008) **[9]**. Their paper looked at two causal mechanisms: normal magneto-ionic refraction from quasi-random elemental patches of ionization with higher electron density than the background plasma (also referred to as "ionospheric roughness") and two-hop ground side-scatter, that is, off the great circle path between transmitter and receiver, such that each hop distance was supported by the MUF at the time. The following is a working hypothesis — I2 arose from one-hop F layer propagation via magneto-ionic refraction from patches of higher ionization, given the following observations and assumptions:

- I2 showed low spectral spreading, which, as a working assumption, we associate with magneto ionic refraction rather than ground side scatter which we assume would show greater spectral spread from multipath.
- The drop in SNR was modest, at 9 dB, and I2 was not always present, which would rule out the ever-present ionospheric scattering mode that would have a much lower SNR, i.e. greater path loss.

Label I3: There was no equivalent in the propagation prediction to I3, present only on 30 December at KA7OEI-1. Two hypotheses, A and B, for I3 are set out below, the first based only on the data at KA7OEI-1, the second including data at ND7M (645 km) and KK6PR (679 km).

Hypothesis A: I3 arose from two-hop E layer propagation, given the following observations / assumptions:

- I3 was present between 0028 UTC and 0258 UTC on 30 December and not at all on 31 December – it was an intermittent mode.
- The closest ionosonde record, at the Idaho National Laboratory, showed a strong blanketing E layer between 0400 UTC and 0645 UTC, peaking at 0515 UTC with an foEs of 6.1 MHz **[10]**. The duration was similar to that of the I3 event, but displaced in time by 3.5 hours. However, we know that "clouds" of E layer activity drift.

Mid-latitude one-hop magneto-ionic refraction from the F2 layer, as in I1, shows low spectral spread. While we have yet to obtain FST4W records from unequivocal E layer propagation our working assumption is that single hop E layer propagation would not induce 16 times the observed spectral spreading of 1F mode I1. Barnum (1968) **[11]** however, found that ground forward-scatter reflections from irregularities caused "severe vertical broadening" of oblique ionosonde records **[10]**. Hence hypothesis A puts forward two-hop E layer propagation with intermediate ground forward scatter as the explanation for cluster I3.

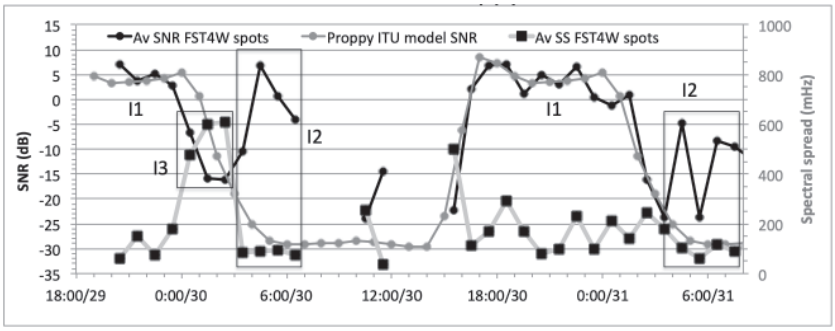

Figure 13 — Time series of observed SNR at KA7OEI-1 (black) with the SNR prediction of *Proppy* (grey) assuming rural noise and FST4W spectral spread (light grey, black squares). The shape and dynamic range of the main daily SNR peak were consistent between the observations and *Proppy*, but *Proppy* did not show the nighttime peak.

Hypothesis B: I3 arose from an above the basic MUF (ABM) mechanism, such as ground (or sea) side-scatter over an F layer two-hop path, not along the great circle, with an unknown geometry, where each hop was supported by the MUF at the time and refraction location. This propagation mode has been discussed in McNamara et al. (2008) **[9]** and summarized in ITU report ITU-R P.2011 **[12]**. Arguments in support of hypothesis B are:

- I3 was present throughout the day and past sunset on 29/30 December 2022 at ND7M (645 km ESE to 0252 UTC) and at KK6PR (679 km N to 0258 UTC). Persistence through daylight hours and presence at orthogonal sites some 1000 km apart argue against hypothesis A's propagation via two-hop sporadic blanketing E layer.
- The intermediate ground side-scatter provides the mechanism for the observed high spectral spreading and the lower SNR over 1F refraction.

ITU Recommendation ITU-R P.533 **[8]** has a simple expression for the excess loss L_m where the operating frequency f is at, or greater than, the basic MUF f_b for path distance D. For D<7000 km and F layer propagation, when $f > f_b$:

$$L_m = 36\left[\frac{f}{f_b} - 1\right]^2 \text{ dB or 62 dB whichever is the smaller.}$$

f_b was calculated for the interval 1830 UTC 29 December 2022 to 0330 UTC 30 December 2022 for paths of 645 km and 679 km corresponding to receivers at ND7M and KK6PR when I3 was present by interpolation of the ionosonde MUFs at 600 km and 800 km from the Idaho National Lab. **Table 2** gives the median excess loss L_m calculated from the above equation for f = 14.097 MHz and the observed median excess loss of I3 over 1F SNR when f_b was over 8 MHz (a 6 h interval). The over 8 MHz criterion avoided large differences attributable to the Idaho Lab f_b not being representative of the midpoints further west as f_b fell rapidly in the evening.

The agreement at KK6PR was (quite frankly) astonishing, given that the 1F SNR was measured the following day, and that antenna response may be different between the 1F great circle path and off-great circle ground side-scatter two hop path(s). The agreement was not as good at ND7M, but the difference of 4 dB is not substantial, and it is in the expected direction, that is, greater L_m at the shorter distance (lower f_b).

The balance of evidence favors hypothesis B — 2F ABM propagation over hypothesis A — sporadic 2E. The 2F ABM hypothesis explains propagation during daylight hours at ND7M and KK6PR as well as after sunset on the 960 km path to KA7OEI-1, and the two briefer periods on the 1525 km path to N6GN/K, as the MUF fell through the operating frequency.

Table 2 – Model and measured median excess loss Lm for paths to ND7M and KK6PR.

Receiver	Path (km)	Model Mdn Lm (dB)	Meas Mdn Lm (dB)
ND7M	645	22.7	26.6
KK6PR	679	22.1	22.4

4210 km transcontinental path over land to WA2TP, Long Island, New York

Label I was, with high certainty, 2F magneto-ionic refraction. Analysis using the *PyLap* ray tracing package **[13]** confirmed the 2F hypothesis; one-hop along 070° from WB7ABP only reaching 2000 km at the December SSN of 103, even at the minimum elevation angle of 2°. The spectral spreading (median 277 mHz) on this 2F path was more than twice that on 1F paths at mid latitudes during quiet geomagnetic conditions (e.g. 73 mHz to N6GN/K).

3762 km seawater path to AI6VN/KH6, Maui

Label I4 was, with high certainty, 2F magneto-ionic refraction as in a *PyLap* ray tracing simulation, **Figure 14 [top]**. The median spectral spreading, 266 mHz, was essentially the same as the 277 mHz on the 2F 4210 km overland path to WA2TP, Long Island.

Label I5 was likely a form of 1F magneto-ionic refraction, given the 83 mHz median spectral spread was very similar to the 1F paths to N6GN/K (73 mHz) and KA7OEI-1 (87 mHz). While a *PyLap* ray tracing at 0645 UTC does show 1F to ~3300 km, **Figure 14 [bottom]**, the 1F path in the simulation was short-lived (tens of minutes) not the four hours observed on 30 December 2022 and, even at 2° elevation, did not quite reach 3762 km.

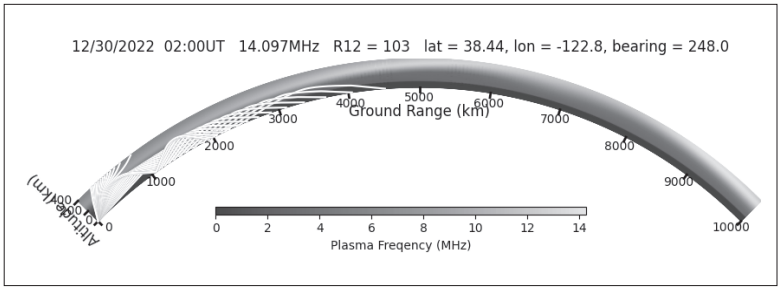

[A]

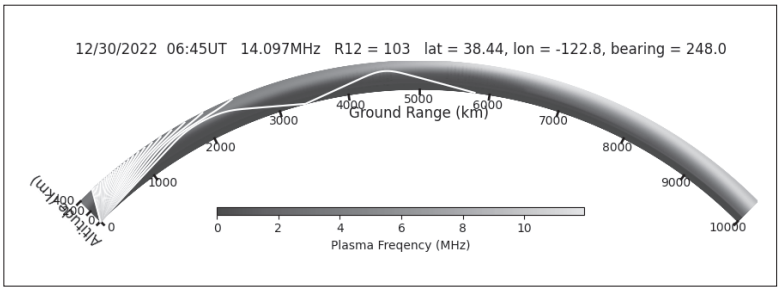

[B]

Figure 14 — [A]: PyLap ray traces showing two-hop propagation from WB7ABP to AI6VN/KH6 at 3762 km on a bearing of 248° during the high SNR period labeled I4 in Figure 11. [B]: PyLap showed short-lived one-hop propagation to over 3000 km was possible around the time the band closed. However, our observations based on the duration of low spectral spread suggested that the one-hop mode persisted for some four hours.

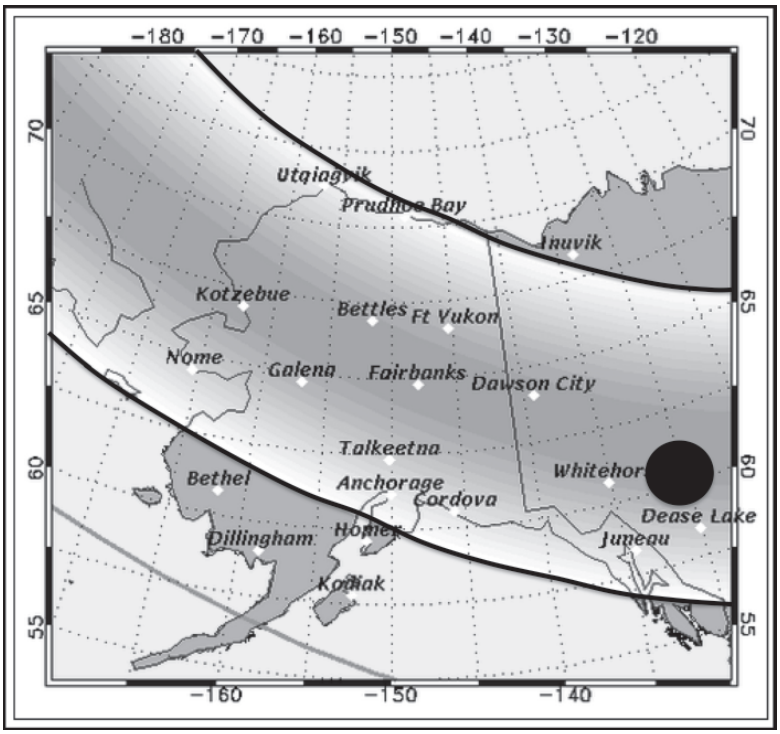

Figure 15 — Map of the position and extent of the Auroral Oval (between the black arcs) on 30 December 2022 from https://www.gi.alaska.edu/monitors/aurora-forecast together with an estimate of the zone for the second hop refraction from the ionosphere for 2F propagation (black circle).

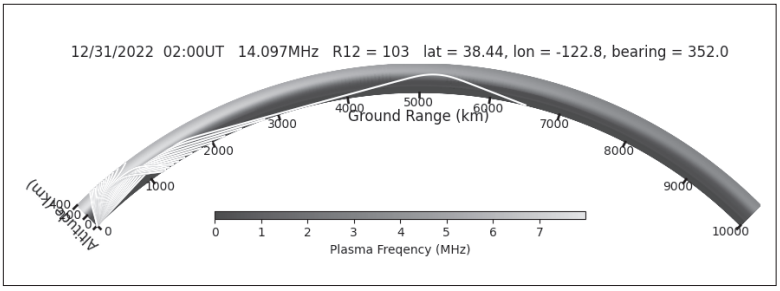

Figure 16 — *PyLap* ray traces showing one-hop propagation from WB7ABP to INUVIK at 3392 km on a bearing of 352° during the low spectral spread period labeled I7 in Figure 12.

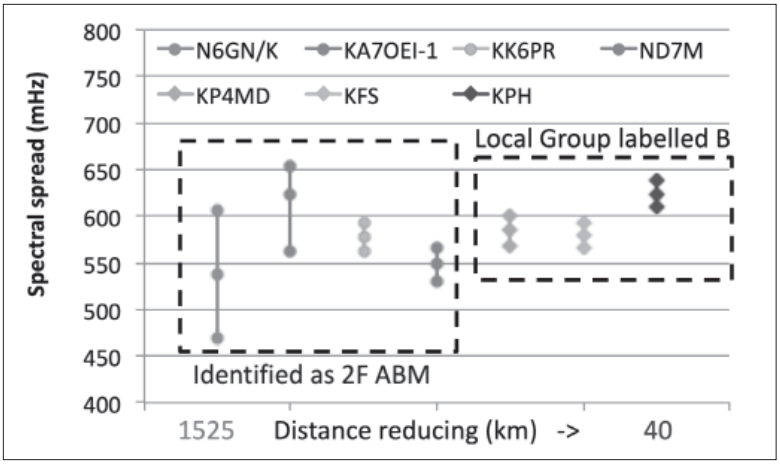

Figure 17 — Median spectral spread with the endpoints at plus and minus one standard error of the median for the four receivers where the mode was identified as 2F ABM propagation together with the medians for clusters B in the Local Group. The implication is that for clusters labeled B the propagation mode was 2F ABM.

In this instance 1F propagation lasted significantly longer than in the *PyLap* model. Hence our conclusion that I5 was 'a form of' 1F refraction where the exact mechanism is not clear.

3392 km into the auroral oval to Inuvik, Northwest Territory, Canada

Label I6 was, with high certainty, 2F magneto-ionic refraction even though the spectral spreading was twice that on mid-latitude paths. Inuvik, Northwest Territory, Canada at 68.35°N is, depending on geomagnetic conditions, either within the Auroral Oval or to its north. **Figure 15** shows the position of the Auroral Oval for 30 December 2022. The black circle shows the estimated position of the refraction by the ionosphere for the second hop of the 2F propagation path. Refraction within the Auroral Oval, even during a quiet period, would likely increase spectral spread on this path. The observed value (500 mHz) was almost double that on mid-latitude 2F paths of similar distance (277 mHz to WA2TP and 266 mHz to AI6VN/KH6).

Label I7 was applied to four out of thirty spots on this path, characterized by their lower spectral spread. Our working assumption is that the propagation mode was 1F. A single hop would have been refracted by the ionosphere south of the Auroral Oval. However, the spectral spreading on this path (137 mHz) was, nevertheless, substantially higher than on 1F mid-latitude paths (e.g. 73 mHz to N6GN/K, 83 mHz to AI6VN/KH6). We attribute this to the downward ray toward Inuvik passing through the Auroral Oval. 1F propagation at the time observed was seen in a *PyLap* ray trace, **Figure 16**.

The Local Group

The original motivation for this study was to identify the modes with labels A, B and C in this local group.

Label B: Our approach of first attributing SNR and spectral spreading clusters to specific propagation modes for distances of over 600 km proved useful when seeking to attribute modes to clusters labeled B. **Figure 17** plots the median spectral spreading together with end points at plus and minus the standard error of the median where we identified the mode as 2F ABM at distances of over 600 km. The median spectral spreading for the clusters labeled B in the Local Group were within the range of spectral spreading for 2F ABM for the more distant receivers. Therefore, our working hy-

pothesis is that the clusters labeled B in the Local Group represent 2F ABM propagation. Unfortunately, we do not have instances of 1F propagation at these shorter distances against which to calculate the SNR reduction for 2F ABM. This was because the MUF at the time was not sufficiently high to support 1F at 14 MHz at these short distances.

Label A: Our working assumption is that clusters labeled A represent ground (or surface wave) propagation, based on the following points:

- Rare (10 out of 177 spots, 6%) and with low SNR at KFS, distance 121 km, and not present at all at KP4MD, distance 133 km, a site with residential rather than rural noise level.
- Present 47% of the time at the closer receiver, KPH, distance 40 km, as a lower SNR, lower spectral spread nighttime mode after the MUF had dropped sufficiently for the SNR from 2F ABM propagation to drop below that of the ground wave. The ground wave was weak as horizontally polarized antennas were used each end.

Label C: We do not have a credible hypothesis for this cluster. The relevant facts are:

- KFS was the only station where this mode was received.
- It was only seen at night.
- Moreover, it was only received on two of the station's four antennas **[14]**: On Omni_A, an omnidirectional TCI530-5-02 log periodic antenna with a nominal gain of 6 dBi, the antenna used in this study, and on the SE sector antenna, a TCI527B "super high gain log-periodic" with a nominal gain of 15 dBi, a front-to-back ratio of 13 dB, and a beamwidth of 64° centered on 135°. The median SNR for cluster C was –21.9 dB on Omni_A (11 spots) and –24.1 dB on the SE antenna (15 spots).
- The mode was not received on the NW sector antenna, a TCI532-4-02 log periodic with a nominal 12 dBi gain directed 278°, or the SW sector antenna, of the same type, directed toward 222°.
- This mode was not present every day, but the cluster labeled A, ascribed to ground wave, was also not present to the same extent every day.
- The median spectral spreading at 288 mMHz on Omni_A was seen on 2F ionospheric paths, but 2F is not considered a credible hypothesis for a nighttime mode over a 121 km path.

Our conjecture is that the cluster labeled C was from multipath ground wave, perhaps involving diffraction and or scattering, perhaps involving the northern Santa Cruz Mountains that

Table 3 – Summary of the attribution to propagation modes for the SNR/spectral spreading clusters identified at the eleven receivers in this study. IR is Ionospheric Roughness, and ABM is Above the Basic MUF — taken to be ground sidescatter, Mdn is the median, and MAD is median absolute deviation. The propagation mode for the cluster identified with label C at KFS remains unknown.

Path	Dist (km)	Initial Label	Mode	Mdn SNR (dB)	MAD SNR (dB)	Mdn SS (mHz)	MAD SS (mHz)
WW6D	2.4	G	Gnd wave	3.0	0.8	5.0	2.7
KPH	40	A	Gnd wave	–11.3	2.3	59	27
		B	2F ABM	–6.8	1.8	624	83
KFS	121	A	Gnd wave	–22.2	0.7	118	48
		B	2F ABM	–9.7	2.4	580	99
		C	Unknown	–21.9	0.5	288	154
KP4MD	133	B	2F ABM	–19.1	2.4	585	97
ND7M	645	I1	1F	1.4	5.7	88	39
		I3	2F ABM	–22.3	3.6	549	67
KK6PR	679	I1	1F	3.8	4.9	69	21
		I3	2F ABM	–16.9	2.7	578	62
KA7OEI-1	960	I1	1F	5.4	3.7	87	38
		I2	1F IR	–3.4	7.2	77	28
		I3	2F ABM	–15.2	1.3	623	76
N6GN/K	1525	I1	1F	–6.2	3.5	67	55
		I2	1F IR	–20.2	4.7	73	30
		I3	2F ABM	–19.4	3.1	538	160
WA2TP	4210	I	2F	–23.2	3.0	277	65
AI6VN/KH6	3762	I4	2F	11.9	2.3	266	83
		I5	1F	–21.7	4.2	83	20
INUVIK	3392	I6	2F	–24.2	2.4	500	101
		I7	1F	–16.4	2.9	137	12

form the spine of San Francisco peninsula immediately inland from KFS. Furthermore, there must be circumstances we have yet to determine or understand that affect when this mode prevails.

Summary of assignment to propagation modes

Table 3 summarizes the assignment of the initial SNR and spectral spreading cluster labels to recognized modes of propagation determined or hypothesized in the preceding sections. The mode labeled C is the only cluster without a credible hypothesis.

Discussion

If only SNR was available, for example from WSPR, it would have been far more difficult to assign the received spots from this experiment to propagation mode with any degree of confidence. SNR alone is so dependent on local conditions at the receiver. This makes it difficult to compare SNR values across sites. It is the combination of the spectral spreading measurement from *FST4W* and the frequency stability of the WB7ABP transmitter and eleven KiwiSDR and ELAD receivers, together with SNR, that has made possible assignment to propagation mode.

Most of the paths showed more than one propagation mode. At times modes alternated over tens of minutes. More often propagation modes followed in succession on a daily cycle as the MUF changed. The degree of separation of the SNR/spectral spreading clusters was surprising, most showing no ambiguity between clusters. This was either because changes between propagation modes were fast, with few intermediate spots, or else there was a clear gap in time between distinct modes. Recognizing the spectral spreading associated with a mode in a clear and unambiguous case made it easier to spot the same mode on a path where, beforehand, there had been no explanation for the propagation mode. This was especially true for the 2F ground side-scatter mode on paths from 40 km to 1525 km. Indeed, experienced radio amateurs consulted did not, before this study, immediately associate this mode with propagation at 14 MHz over these paths. Further insights could come from using *FST4W* and beam-forming, electronically-rotated receive antennas with a step-rotating transmit antenna; a modern form of the 'Pinwheel' technique of the early 1960s that produced many observations of deviated-path signals **[15]**.

The method described proved useful for determining propagation modes on paths across continental North America before, during and after the 14 October 2023 annular eclipse **[16]** and the 8 April 2024 total solar eclipses as changes in solar flux impact ionosphere dynamics and structure.

The mode labeled C, only observed occasionally on two of the antennas at KFS, a path of 121 km, remains a mystery. It is possible that longer time series, making full use of the directionality from the four receive antennas at KFS, and systematically altering the heading of the transmit Yagi antenna may lead to a better characterization and subsequently to an attribution for this mode.

Far from being a beacon mode of interest only at LF and MF by measuring spectral spread FST4W is an excellent propagation analysis tool at HF.

Acknowledgement

The author is grateful to Lynn Rhymes, WB7ABP, for providing the precise frequency *FST4W-120* transmissions and to the following for providing *FST4W* spots: Doug Bender, WW6D, the Maritime Radio Historical Society, KPH; Craig McCartney, W6DRZ; Globe Wireless Radio Services and KFS Radio Club, KFS; Carol Milazzo, KP4MD; Dennis Benischek, ND7M; Rick Wahl, KK6PR; Clint Turner, KA7OEI; Glenn Elmore, N6GN; Rob Robinett, AI6VN; Bryan Klofas, KF6ZEO for Inuvik; and Tom Paratore, WA2TP. This study could not have been performed without the *WsprDaemon* software package from Rob Robinett and *FST4W* by the WSJT-X development team.

Gwyn Griffiths, G3ZIL, was first licensed in 1970 as GW3ZIL. He spent his career developing instruments for marine scientists, becoming UK National Oceanography Center's Chief Technologist and Professor of Underwater Systems at Southampton University. Since retiring in 2012 he has returned to amateur radio, concentrating on using WSPR and FST4W and data analysis to understand and document HF band noise and propagation modes. He is an associate member of the Radio Society of Great Britain Propagation Studies Committee.

References

[1] **github.com/rrobinett/wsprdaemon**

[2] **wsprdaemon.org/** for guides on how to access the database

[3] TAPR/ARRL Digital Communications Conference Proceedings at **files.tapr.org/meetings/DCC_2022/2022%20DCC1.pdf**.

[4] Available via **wsprdaemon.org/fst4w.html**

[5] **fetzerch.github.io/2016/07/03/grafana-sunandmoon-datasource/** from zip file

[6] G. Griffiths, R. Robinett, and G. Elmore, 2020. Estimating LF-HF band noise while acquiring WSPR spots. *QEX*, ARRL, Sept./Oct. 2020.

[7] **soundbytes.asia/proppy/p2p**

[8] **www.itu.int/dms_pubrec/itu-r/rec/p/R-REC-P.533-14-201908-I!!PDF-E.pdf**

[9] L.F. McNamara, et al., 2008. Nighttime above-the-MUF HF propagation on a midlatitude circuit. *Radio Science*, 43(2).

[10] **lgdc.uml.edu/common/DIDBDayListForYearMonthAndStation?ursiCode=IF843&year=2022&month=12**

[11] J.R. Barnum, 1968. Mixed-Mode Oblique Ionograms: A Computer Ray-Tracing Interpretation. Stanford University Ca., Stanford Electronics Labs. available at **apps.dtic.mil/sti/pdfs/AD0845620.pdf**.

[12] **www.itu.int/dms_pub/itu-r/opb/rep/R-REP-P.2011-1997-PDF-E.pdf**

[13] **https://github.com/hamsci/pylap**

[14] **www.klofas.com/blog/2021/picoballoon-launch-11/KFS-KiwiSDR.pdf**

[15] F.H. Dickson, and R. Silberstein, 1964. Great-Circle and Deviated-Path Observations on CW Signals Using a Simple Technique. Army Signal Radio Propagation Agency, Fort Monmouth NJ, available at **https://apps.dtic.mil/sti/pdfs/AD0603772.pdf**.

[16] G. Griffiths, 2024. Analysis of changes to propagation and refraction height on specific paths induced by the 14 October 2023 eclipse. HamSci 2024 Workshop proceedings at **https://tinyurl.com/4nuy9veb**